Colloids and Surfaces A: Physicochemical and Engineering Aspects 709 (2025) 136074

Contents lists available at ScienceDirect

Colloids and Surfaces A: Physicochemical and Engineering Aspects

journal homepage: www.elsevier.com/locate/colsurfa

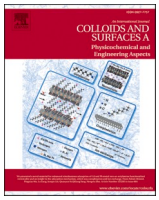

Preparation of hydrogel-supported giant vesicles via a lipid-coated hydrogel transfer method with electrostatic interaction

Daisuke Saeki [a,b,*], Kazuyuki Honma [b], Yukihisa Okumura [b]

[a] Research Initiative for Supra-Materials (RISM), Interdisciplinary Cluster for Cutting Edge Research, Shinshu University, 4-17-1 Wakasato, Nagano 380-8553, Japan
[b] Department of Engineering, Graduate School of Science and Technology, Shinshu University, 4-17-1 Wakasato, Nagano 380-8553, Japan

HIGHLIGHTS

- A lipid-coated hydrogel transfer method was develoeped to prepare HydroGel-Supported Giant Vesicles (GSGVs).
- Charged hydrogel particles of uniform size were used as a unique template and internal aqueous phase.
- The size of the obtained GSGVs corresponded to the template hydrogel particles.
- The obtained GSGVs had the fluidic lipid membranes and retained dextran larger than 40 kDa.

GRAPHICAL ABSTRACT

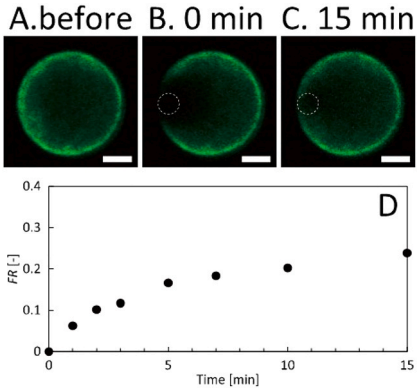

ARTICLE INFO

Keywords:
Giant vesicles
Hydrogel
Lipid bilayer
Oil-in-water interface

ABSTRACT

In this study, we developed a preparation method for novel hydroGel-Supported GVs (GSGVs) via a modified oil-in-water (O/W) interface transfer method, using charged cross-linked hydrogel particles of uniform size as a unique template and the internal aqueous phase. The commercial charged hydrogel particles electrostatically adsorbed lipids with the opposite charge on their surface in an oil phase. By centrifugation, the particles were transferred into the lower aqueous phase through the O/W interface adsorbing the lipid molecules and were transformed to GSGVs. In the combination of cationic lipids and anionic hydrogel particles, the adsorbed lipid molecules covering the particles were detected by the fluorescent microscope observation, and the lipid layer had lateral diffusivity shown by the fluorescence recovery after photobleaching (FRAP) assay. The obtained particles had the size corresponding to the template hydrogel and retained fluorescent dextran larger than 40 kDa in the hydrogel core. These results demonstrated the formation of a new type of GSGVs composed of a pre-defined hydrogel core and lipid membrane.

* Corresponding author at: Research Initiative for Supra-Materials (RISM), Interdisciplinary Cluster for Cutting Edge Research, Shinshu University,4-17-1 Wakasato, Nagano 380-8553, Japan.
E-mail address: Japan.dsaeki@shinshu-u.ac.jp (D. Saeki).

https://doi.org/10.1016/j.colsurfa.2024.136074
Received 8 October 2024; Received in revised form 15 December 2024; Accepted 27 December 2024
Available online 30 December 2024

1. Introduction

Giant vesicles (GVs), which consist of a micrometer-sized internal aqueous core and covering a lipid bilayer membrane, have the size and primary membrane structure similar to biological cells, and have been used as models in the functional reconstruction of the cell membrane [1], the construction of artificial cells [2,3], microbioreactors [4,5] and biosensors [6]. In those applications, the size uniformity, encapsulation efficiency and stability of GVs are essential for the reliable construction and the following quantitative analysis of the systems.

The two most commonly used methods to form GVs are the gentle hydration and the electroformation [7]. Both methods can easily yield GVs using simple equipment and no organic solvents. The known difficulties with those methods are that the size of the obtained GVs is often not uniform, and the encapsulation efficiency is strongly affected by the molecular weight of substances to be encapsulated [8]. As an alternative method, an inverted emulsion method (oil-in-water (O/W) interface transfer method), in which water droplets dispersed in an oil phase containing lipid molecules are transformed to GVs by transferring the droplets into another external aqueous phase through a lipid monolayer formed at the O/W interface between the oil and the external aqueous phases and are transformed to GVs, has been reported [9–13]. With this method, high encapsulation efficiency can be achieved while the size of the obtained GVs still depends on that of the pre-formed W/O droplets [13], which are usually unstable and heterogeneous. In the past decade, fine microfabrication technology such as microcontact printing combined with the electroformation [14] or phase manipulation by microfluidics [15–18] has enabled the precise size control of GVs. Especially, the microfluidics allows GV formation with the uniform size distribution and highly efficient encapsulation [17], which is difficult by the conventional methods. However, these microfabrication methods require sophisticated equipment.

Meanwhile, simple GVs are composed of a self-standing lipid bilayer membrane and are inherently vulnerable to mechanical or chemical stress resulting in their short lifetime [19]. The improvement of the stability of GVs is desired for their practical use but still remains a considerable challenge. Biological cell membranes have some backbones such as cytoskeletons and/or cell walls to support their lipid bilayers, achieving the structure retention and high mechanical stability [20]. Introducing backbone mimics to GVs is efficacious in improving the stability [19,21,22]. To date, several studies of GVs supported on spherical hydrogel particles (hydroGel-Supported GVs; GSGVs) have been reported [10,23–28]. A GSGV has a hydrogel core particle that works as an internal aqueous phase and supporting hydrophilic polymeric structure mimicking the backbone of biological cell membranes. Previously, GSGVs preparations by the vesicle contact method using commercial hydrogel particles [23–26] and the O/W interface transfer method combined with the *in situ* gelation of water-in-oil (W/O) droplets have been reported [10,18,27,28]. The former confirmed the adsorption of lipid molecules on the particle surfaces, while the detailed encapsulation behavior such as a variety of applicable molecules wasn't given. The latter has some restrictions on the size uniformity or complicated preparation process. In both cases, the evidence of a planar lipid bilayer structure including the lipid fluidity was not confirmed sufficiently. Thus, the behavior of the GSGVs obtained in these previous studies was not necessarily satisfactory, and there still is a need for a novel approach to GSGV construction.

In this study, we proposed a novel preparation method of GSGVs, lipid-coated hydrogel transfer method, illustrated in Fig. 1. The method is based on the O/W interface transfer method previously reported [10] but uses charged hydrogel particles in place of water droplets. Charged lipid molecules are adsorbed on the oppositely charged surface of the hydrogel particle in an oil phase, forming a lipid monolayer (Fig. 1A). In this stage, the particle assists as a template to assist the formation of the monolayer, which is to be the inner leaflet of the lipid membrane in the GSGV. And the particle also works as a template to fix the size of the aqueous core, so the GSGV. When the hydrogel particle sinks into the lower external aqueous phase by the specific gravity difference through the O/W interface that has another pre-formed lipid monolayer (Fig. 1B to C), the two monolayers are combined to form a single bilayer covering the particle (Fig. 1D), and the GSGV is obtained. In the present study, this scheme was tested using commercial cationic or anionic hydrogel particles of uniform size, and the effects of the electrostatic interaction between lipid molecules and hydrogel particles on the GSGV formation were investigated. Furthermore, the lipid fluidity on the particle surface and the encapsulation of a water-soluble substance into the internal aqueous phase were evaluated to confirm the formation of a lipid bilayer structure on the particle surface.

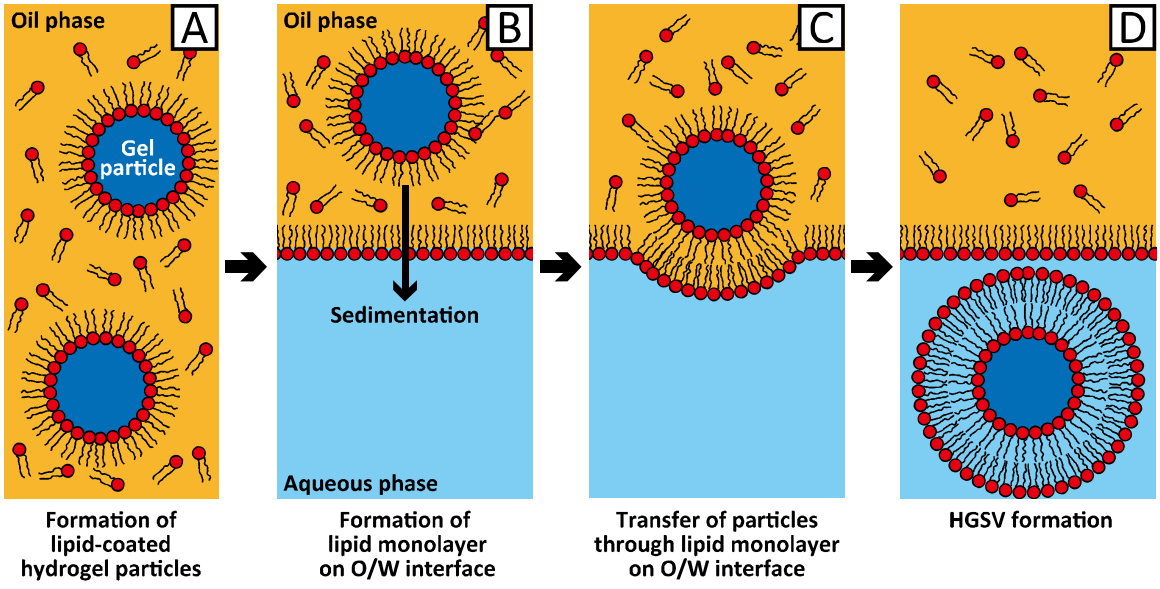

Fig. 1. Schematics of the formation of hydrogel-supported giant vesicles (GSGVs) via the lipid coated hydrogel transfer method, a modified oil-in-water (O/W) interface transfer method used in this study.

2. Experimental section

2.1. Materials

All chemicals were purchased from Fujifilm-Wako Pure Chemical Industries (Osaka, Japan) unless specified otherwise, and used as received without further purification. Aqueous solutions were prepared using Milli-Q water (>18.2 MΩ cm; Merck; Darmstadt, Germany). Chloroform and hexane were selected as an oil phase because they were commonly used to solubilize lipids. Q Sepharose High Performance and SP Sepharose High Performance (GE Healthcare, Chicago, USA; median diameter = 34 μm, exclusion limit = 4 x 10^3 kDa) were used for cationic and anionic template hydrogel particles of GSGVs, respectively. The specific gravity of these hydrogel particles was higher than that of any aqueous phase used in this study. 1-Palmitoyl-2-oleoyl-*sn*-glycero-3-phosphocholine (POPC), 1,2-dioleoyl-*sn*-glycero-3-phosphoglycerol sodium salt (DOPG), and 1,2-dioleoyl-3-trimethylammonium propane chloride (DOTAP) were purchased from NOF (Tokyo, Japan) and used as zwitterionic, anionic, and cationic lipids, respectively. To visualize lipid adsorption onto the particles, 1,1'-dioctadecyl-3,3,3',3'-tetramethylindocarbocyanine perchlorate (DiI) and *N*-(fluorescein-5-thiocarbamoyl)-1,2-dihexadecanoyl-*sn*-glycero-3-phosphoethanolamine, triethylammonium salt (Fluoresceine-PE) were obtained from Biotium (Fremont, USA) and Setareh Biotech (Eugene, USA), respectively. Calcein was purchased from Nacalai Tesque, Kyoto, Japan. Fluorescein isothiocyanate-labelled dextran (FITC-dextran; molecular weight = 3–5, 10, 40, 70 kDa) was obtained from Merck and used to evaluate the encapsulation capability as a model of water-soluble polymer.

2.2. GSGV formation via an O/W interface transfer method

Hydrogel particles were collected on a hydrophilic PTFE filter (Omnipore JCWP; 10 μm pore size; Merck) from their commercially obtained suspension by vacuum filtration using an aspirator and redispersed in a Tris buffer (10 mmol/L tris(hydroxymethyl)aminomethane and 150 mmol/L NaCl; pH adjusted to 7.0 by HCl) to equilibrate the internal aqueous phase of the particles with the buffer. When necessary, 0.2 mmol/L calcein was in the buffer to visualize the internal aqueous phase of the template particles. Next, 60 μL of the particle dispersion was vacuum-filtrated again to remove most part of the external aqueous phase, and about 8–9 mg of the particles were obtained. Then, 1.0 mL of an oil solution containing 70 μmol/L lipids and 0.35 μmol/L fluorescent lipids in chloroform/hexane (1/4 by vol.) or hexane was added to the particles in a 2 mL microtube. Cationic DiI was used with the cationic hydrogel and anionic Fluoresceine-PE with the anionic ones to prevent the interaction of the fluorescent lipids with the gel from being electrostatically preferred over other membrane lipids. The mixture was sonicated for 5 min using a sonication cleaner (2510; Branson; Brookfield, USA) and vortexed at 1200 rpm for 2 h to disperse the particles into the oil solution. The obtained dispersion was gently poured onto a layer of 0.4 mL of another oil solution of the same composition in 2 mL microtube, which was placed on 0.4 mL of the Tris buffer and left for 2 h in advance to allow adsorption of the lipid molecules at the oil/water (O/W) interface. To the upper oil layer in the microtube, the obtained particle dispersion was gently poured. Then, the hydrogel particles in the upper oil solution were transferred into the lower Tris buffer through the O/W interface by centrifuging for 10 min at 300 G for the cationic hydrogel particles or at 120 G for the anionic ones, respectively, using Centrifuge 5430 R (Eppendorf; Hamburg, Germany). Most of the upper supernatant oil solution was manually removed, and the residual oil phase was eliminated entirely from the obtained aqueous dispersion by evaporation using a vacuum pump for 1 h. To wash the particles, 0.15 mL of the obtained suspension was mixed with 1.25 mL of the Tris buffer and centrifuged for 30 s at 240 G, and 1.0 mL of the supernatant was removed. This washing process was repeated five times.

2.3. Observation of lipid membranes

To confirm the adsorption of the lipid molecules on the particles, the obtained dispersion was poured into a flat quartz cell with a 1-mm light path (Type 20/C/Q/1, Starna scientific, UK), and observed with on an inverted optical microscope (IX50; Olympus, Tokyo, Japan) equipped with a fluorescent observation module (IX-FLA; Olympus). U-MWIG and U-MNIBA (Olympus) were used as the filter sets to detect DiI and Fluorescein-PE, respectively. To detect the lipid molecules on the particles, the dispersion was also inspected with a confocal laser scanning microscope (CLSM; FV1000; Olympus).

2.4. Evaluation of ζ-potential

The ζ-potential of the particles was measured by using electrophoretic light-scattering apparatus (Zeta sizer Nano ZS, Malvern Panalytical, UK).

2.5. Evaluation of particle diameter distribution

The particle diameter distribution was evaluated by measuring the diameters of randomly selected 100 particles on the microscopic images. The diameters were categorized every 2.5 μm.

2.6. Evaluation of lipid fluidity

The fluidity of the lipid molecules on the particles was evaluated by a fluorescence recovery after photobleaching (FRAP) assay using the CLSM [29]. The focus was adjusted to the cross-sectional center of the particles. The fringe of the particle was photobleached with 495-nm or 543-nm laser beam of 7-μm diameter, and fluorescent field images were taken. The fluorescence intensities of the circular bleached area (I_b) and the circular unbleached area (I_r), which is the area far from the bleached area, were obtained from the fluorescent field images using Image J software (NIH, Bethesda, MD, USA). The relative fluorescence intensity ($RI = I_b/I_r$), and fluorescence recovery ratio ($FR = (RI - RI_0)/(1 - RI_0)$), were calculated.

2.7. Evaluation of encapsulation

To evaluate the encapsulation capability and the possible defect in the lipid membrane of the obtained GSGVs, calcein or fluorescent dextrans of various molecular weights were tried to be encapsulated in the GSGVs. The GSGVs were similarly prepared using a 0.7 wt% FITC-dextran dissolved in the Tris buffer as the internal aqueous phase of the hydrogel particles. The encapsulated FITC-dextran was detected using the IX50 with the U-MNIBA filter set.

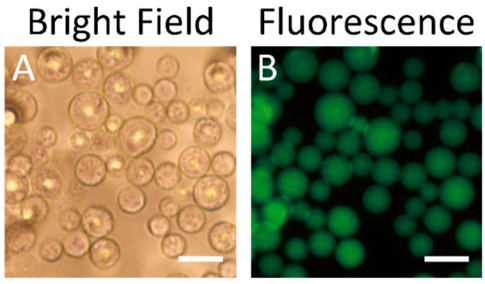

Fig. 2. Microscopic images of the calcein-containing template gel particles dispersed in lipid containing chloroform/hexane. Bars indicate 50 μm.

3. Results and discussion

3.1. Confinement of the aqueous phase in gel particles

Fig. 2 shows the microscopic images of the calcein-containing template particles dispersed in chloroform/hexane. From Fig. 2A and B, the template particles containing calcein were observed in the lipid-containing oil phase like dispersed W/O droplets obtained by sonication. Although the particles were subjected to the sonication and vortexing, no coalescence of the aqueous phases of multiple particles or no deterioration of the particle morphology was visible. The aqueous phase was well confined in the particle. This provides mechanically robust and physicochemically stable aqueous cores that are required in the first step of our GSGV formation process as illustrated in Fig. 1A.

3.2. Effects of the organic solvents

We tested our GSGV preparation method with two different organic solvents, chloroform/hexane and hexane. Many ionic lipids including the ones used in this study show higher solubility to relatively polar chloroform than non-polar hexane, and a chloroform/hexane mixture has been widely used as a solvent for ionic lipids.

When our GSGV preparation method was used with the cationic hydrogel particles dispersed in the chloroform/hexane solution of zwitterionic POPC, they hardly showed fluorescence from the membrane marker DiI (Fig. 3A and B) on the particles and had no lipid layer. When we changed the organic solvent used in the preparation from chloroform/hexane to hexane, the strong fluorescence was seen from the whole particles indicating the adsorption of the lipid molecules onto the particles (Fig. 3C and D).

The lack of the lipids on the particle with chloroform/hexane suggests the failure in the last stage of the GSGV preparation (Fig. 1D). In the present scheme, the affinity of relatively polar chloroform to ionic lipids could rather have worked as a disadvantage by preventing sufficient monolayer formation at the oil/water interface. In non-polar hexane with less affinity to ionic lipids, the lipid molecules would more likely to be concentrated at the interface than in the bulk hexane phase, facilitating the monolayer formation and the success in the last stage of the GSGV formation.

The results indicate that hexane is suitable for the presented concept. In the following experiments, hexane was used as the organic solvent.

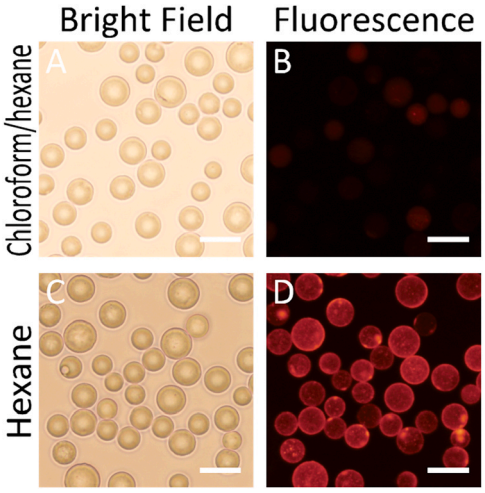

Fig. 3. Microscopic images of the GSGVs obtained by the lipid-coated hydrogel transfer method using POPC, cationic template particles, and chloroform/hexane (A and B) or hexane (C and D) as organic solvents. Bars indicate 50 μm.

3.3. Effect of the electrostatic interaction between hydrogel particles and lipid molecules

In our methods, the lipid-coated hydrogel transfer method, lipid molecules adsorb on the surface of hydrogel particles via electrostatic attraction. Fig. 4 shows the microscopic images of the particles obtained by the O/W interface transfer method using the various combinations of the lipids and hydrogel particles. When combining the lipids with the hydrogel particles of the opposite charge, the obtained particles showed fluorescence from the fluorescent lipids (Fig. 4C and D). Significantly, the fluorescence on the particle surface was stronger than that from the inside of the particles, indicating the adsorption of the lipids on the surface and the GSGV formation. On the other hand, the particles prepared with the combination of the lipid and the particles of the same charge had very little fluorescence (Fig. 4A and F); therefore, few lipid adsorbed. POPC, which is a zwitterionic lipid but possesses a negative charge due to the orientation of polar heads of phospholipid [30], gave the images similar to anionic POPG (Fig. 4B and E), suggesting that the effective charge should determine the GSGV formation. Although the structures of the polar head groups among the three lipids examined are largely different, the results can be explained simply in terms of the electrostatic charge. Table 1 shows the ζ-potential of the template hydrogel particles and GSGVs. The positive surface charge of the cationic hydrogel particles changed to a negative value by the O/W interface transfer method with zwitterionic POPC or anionic POPG, indicating the coating of the particle surface with oppositely charged lipids. In the case of the anionic hydrogel particles, the absolute value of the surface charge decreased to a neutral value. The cationic DOTAP neutralized the surface charge of the anionic particles. These facts strongly suggest that the electrostatic attraction should mainly cause the adsorption of the lipid molecules on the particle surface and be essential for the GSGV formation by the present method.

Fig. 5 shows the particle diameter distribution of the prepared GSGVs using DOTAP and the anionic hydrogel particles obtained from the fluorescent image partially shown in Fig. 4D. The distribution for the GSGVs agreed well with the template hydrogel particles. The average diameter and standard deviation also had the same value. These facts indicate the size of the obtained GSGVs reflected that of the template particles In the case of the conventional O/W interface transfer method using aqueous droplets as templates, the optimization of the centrifugation condition requires to obtain the size corresponding templates, and the size of GVs tends to show broad distribution and/or to change over time by growth or coalescence because of the low mechanical/physicochemical stability of the W/O droplets [10,28]. In this study, the rigid and uniform hydrogel particles can determine the shape of the

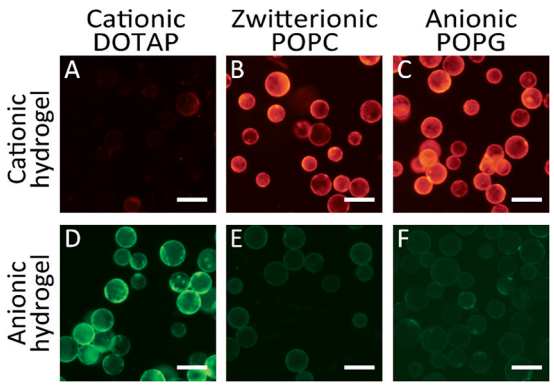

Fig. 4. Microscopic images of the gel particles obtained by the lipid-coated hydrogel transfer method using the various combinations of the lipids and hydrogel particles. Cationic DiI (red) and anionic Fluorescein-PE (green) were used as fluorescent lipids for cationic and anionic hydrogel particles, respectively. Bars indicate 50 μm.

Table 1
ζ-potential of the template hydrogel particles and GSGVs.

Template hydrogel	Lipid	ζ-potential [mV]
Cationic	-	20.3
Anionic	-	−31.7
Cationic	POPG	−12.2
Cationic	POPC	−4.8
Anionic	DOTAP	−5.8

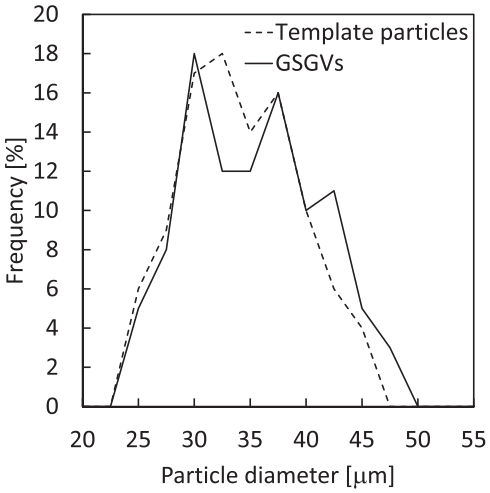

Fig. 5. Particle diameter distribution of the GSGVs obtained with cationic DOTAP and the anionic hydrogel particles. The particle diameters of 100 particles randomly selected were counted. The average diameters and standard deviation of the template hydrogel particles (dotted line) and GSGVs (solid line) were 33.0 and 34.0 μm, and 5.2 and 5.8 μm, respectively.

internal aqueous phase and keep the morphology during the transformation to the GSGVs in the present O/W interface transfer process, resulting in the superior size control of GSGVs to the conventional transfer method.

The GSGVs prepared by the present method are robust. Both the shape of the aqueous core and the lipid membrane of the GSGVs were maintained even after a five-times washing process using centrifugation. The robustness originates from the mechanical stability of the hydrogels and the electrostatic attraction between the hydrogels and the lipid membrane. This clearly demonstrates the advantage of our present method over the conventional one.

3.4. Lateral diffusivity of lipid molecules on surface of hydrogel particles

When planar lipid bilayers form on hydrogel particles, the lipid molecules have lateral diffusivity[31]. To clarify the state of the lipid molecules adsorbed on the surface of the prepared particles, the lateral diffusivity of the lipid molecules was evaluated by the FRAP assay. Fig. 6A to C shows the CLSM images from the FRAP experiment. The prepared particles before the photobleaching had strong fluorescence at the circular rim in Fig. 6A, indicating the lipid molecules adsorbed specifically on the particle surface. After the photobleaching, the fluorescence was entirely disappeared (Fig. 6B) and then recovered over time (Fig. 6C). The fluorescence outside the laser spot also slightly bleached, probably due to the laser scattering in the particles. The recovery of the fluorescence was also visible in this region. Fig. 6D shows the time course of *FR* analyzed from the CLSM images. The value of *FR* increased with time. These results suggest that part of the lipid molecules adsorbed on the surface should be in the laterally diffusive state, namely, the planar lipid bilayer.

The lateral diffusion coefficient of lipid molecules (D, cm^2/s) was briefly calculated with the equation $D = 0.22\, w^2/t_{1/2}$, where w and $t_{1/2}$

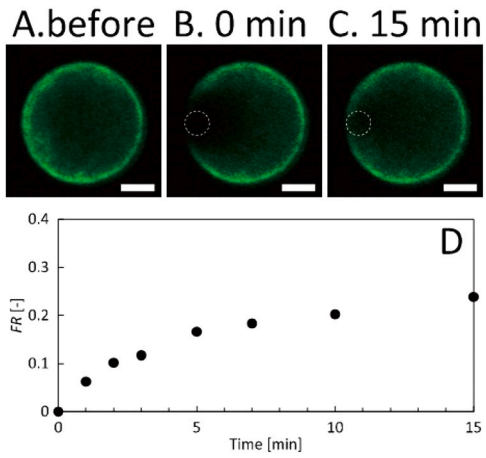

Fig. 6. Fluorescence recovery after photobleaching (FRAP) assay of the GSGVs obtained with cationic DOTAP and anionic hydrogel particles. (A to C) Confocal laser scanning microscopic (CLSM) images before (A), 0 min (B) and 15 min (C) after the photobleaching. Dotted circles mark the laser spots. Bars indicate 10 μm. (D) Time course of the fluorescence recovery ratio (*FR*) after the photobleaching.

are the bleached radius and the time of which *FR* reach 50 % of the equilibrium value, respectively [29]. Assuming that the lipid molecules entirely diffused and that the bleached area reached equilibrium at 15 min after the photobleaching, $t_{1/2}$ was about 3 min, and the calculated D was 1.5×10^{-10} cm^2/s. This value is much lower than the reported one for a POPC SLB on flat glass surface [32]. The apparently low lateral diffusion coefficient suggests that the lateral diffusivity of the lipid molecules on the inner leaflet of the lipid bilayer could likely be restricted by the electrostatic attraction with the particle surface [33–35].

The observed maximum value of *FR* was 23.8 % after 15 min. In theory, if a planar lipid bilayer is formed on the surface and all lipid molecules in the inner leaflet of the lipid bilayer are immobilized by the strong electrostatic interaction with the charged gel surface, only all the lipid molecules in the outer leaflet can diffuse laterally and then *FR* ultimately reaches 50 %. The maximum value of *FR* observed in this assay was lower than the theoretical one. This result suggests that the lipid layer on the particle surface partially contained non-lamellar structures, such as aggregates or reverse micelles which could not diffuse laterally.

3.5. Encapsulation of a water-soluble polymer into the internal aqueous phase of GSGVs

When the prepared particle is entirely covered with defect-free lipid membrane on the surface, the internal aqueous phase is a closed space and can keep water-soluble molecules from freely leaking to the external aqueous phase [8]. Fig. 7 shows the encapsulation of FITC-dextran, model water-soluble molecules, in the GSGVs prepared with the anionic particles. When cationic DOTAP was used as the lipid, the fluorescence of FITC-dextran was mainly detected in the interior of the particles (Fig. 7B). This indicates the FITC-dextran in the hydrogel at the first step of the GSGV preparation process (Fig. 1A) was still held in the particles. On the other hand, no fluorescence was detected from the particles prepared without lipid (Fig. 7A), with POPC (Fig. 7C) or POPG (Fig. 7D). The results are consistent with the presence/absence of the lipids on the hydrogel particle surface shown in Fig. 4. The combination of template particles and oppositely charged lipids enables the formation of the lipid membrane which restricts the diffusion of the FITC-dextran from the interior to the exterior of the particles.

To further evaluate the integrity of the GSGVs obtained with the above combination of the lipid and the gel particles, the effect of the

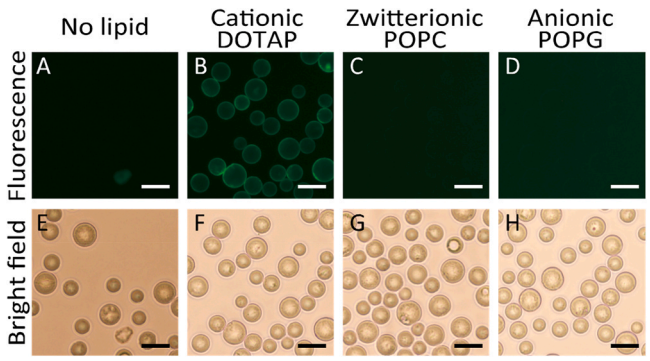

Fig. 7. Encapsulation into the GSGVs prepared with the anionic hydrogel particles. FITC-dextran of 70 kDa was in the aqueous phase of the hydrogel particles in the GSGV preparation. Bars indicate 50 μm.

molecular weight of the FITC-dextran on the encapsulation was investigated (Fig. 8). When FITC-dextran of larger than 40 kDa was used, the fluorescence from the FITC-dextran was mostly confined in the interior of the prepared particles (Figs. 7B and 8A). The results suggest that relatively large biological molecules, such as proteins and nucleic acids, could be encapsulated. FITC-dextran and hydrogel particles used in this study are anionic, indicating FITC-dextran was encapsulated into the particles not via the electrostatic attraction reported previously [23] but via the physical barrier of lipid membranes. The presented method is also applicable to the encapsulation of enzymes used in the *in situ* gelation method [18,28]. Meanwhile, with FITC-dextran of 10 or 3–5 kDa, the GSGVs showed no fluorescence (Fig. 8B and C). The lipid membrane of the prepared particles had some defects permeable to small molecules less than 10 kDa. The hydrodynamic diameters (d, nm), calculated from the equation $d = 0.066 \times Mw^{0.463}$ [36], of 10 and 40 kDa of dextrans correspond to 4.69 and 8.92 nm, respectively. The defect size of the lipid membrane of the prepared GSGVs is estimated to be in this range, which is much smaller than the pore size of the hydrogel particles, 75.2 nm, calculated from the exclusion limit of the particles using the same equation. A large part of the lipid membrane likely covered the pores or openings on the surface of the hydrogel particle as a self-standing membrane.

The defects in the bilayer membrane covering the particles are likely to be present as non-bilayer structures, and this is consistent with the result of the FRAP study indicating the existence of the lipids that lacked the lateral diffusivity. One possible explanation for the cause of the defect formation is that the lipid bilayer formation is incomplete in the last step of the O/W interface transfer process (from Fig. 1C to D). In this step, the hydrogel particle covered with a lipid monolayer is transferred into the external aqueous phase through another lipid monolayer pre-

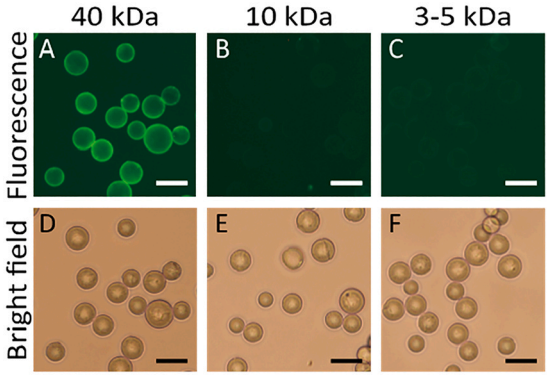

Fig. 8. Effect of the molecular weight of FITC-dextran on the encapsulation into the GSGVs prepared with cationic DOTAP and anionic hydrogel particles. Bars indicate 50 μm.

formed at the O/W interface between the oil and the external aqueous phases, pushing out the oil phase and combining the two monolayers into a planar lipid bilayer (Fig. 1C). A part of the pre-formed monolayer at the interface is consumed to be the outer leaflet of the lipid bilayer covering the particle, while the extra lipids in the oil phase are provided to the interface to regenerate the monolayer (Fig. 1D). When the rate of the regeneration is slower than the consumption, the particle fails to obtain enough amount of the monolayer to complete the bilayer formation. This may result in defects in the bilayer membrane. For instance, if the rate for the particle to pass through the O/W interface was fast and the adsorption of the lipid to the interface was slow, defects in the lipid bilayer could occur.

Another possible explanation is that a self-standing part of the lipid bilayer covering the large pores of the template particles may collapse during and/or after the GSGV formation process. Due to the lack of sufficient support from the hydrogel network, the part of the bilayer membrane may be fragile as that is the case for the GVs prepared using the water-droplets[9].

At the present moment, the defect formation may restrict the application of the GSGVs. Previously, with a similar concept of using pre-prepared template particles, Grossutti *et al.* obtained GSGVs by contacting commercial hydrogel particles for gel permeation chromatography with small vesicles via electrostatic attraction [24–26]. Although the coated lipid layer on the particles acted as some barrier against terbium ions, the layer showed leakage [25,26] and had no lipid fluidity [26]. Also, Helwa *et al.* reported the vesicle contact method using hydrogel particles that polymerized themselves as templates, but the lipid membrane of their GSGVs had defects [23]. These previous studies illustrate the difficulty in obtaining a defect-free bilayer membrane on GSGVs. Although this study shows that the GSGVs prepared by the presented method are no exception and still have some defects of several nanometers and partial non-bilayer structures in their membrane, the study also provides the direction to the possible remedies. Our further investigation includes, for example, optimizing the operation conditions such as the rate for the particles to pass through the interface, using hydrogel particles, specialized for this presented method, with lower exclusion limits or denser surfaces to reduce the size of the pore and the self-standing part of the bilayer membrane, and so on.

The presented method has advantages on the simplified preparation process and size uniformity over the *in situ* gelation method [10,27,28]. In addition, the obtained GSGVs showed lipid fluidity, which is essential for incorporating membrane proteins into lipid membranes and expressing their function, unlike the other studies of the particle-templating method [23–26]. These would give GSGVs significant potential as a biomimetic spherical space and lipid membrane scaffold.

4. Conclusions

By modifying the conventional O/W interface transfer method, we designed the lipid-coated hydrogel transfer method and prepared novel GSGVs with commercial charged hydrogel particles as the aqueous core. The obtained GSGVs demonstrated both the robustness and the size control surpassing those of GVs prepared by the conventional O/W interface transfer method. The closed lipid membrane of the GSGVs had partially the bilayer membrane structure, and the GSGVs retained molecules larger than 40 kDa in their hydrogel core.

The lipid-coated hydrogel transfer method is a promising way to prepare GSGVs with their morphology and stability pre-defined by the template hydrogel particles. The robustness and the superior size control of the GSGVs demonstrated in this study break the limitation imposed by the fragility and instability of simple GVs composed of only a lipid membrane. Furthermore, the present method may be used with various pre-designed, functionalized hydrogel particles[37]. This can open a convenient way to add extra functions to GSGVs to create advanced GVs with advanced features.

CRediT authorship contribution statement

Daisuke Saeki: Writing – review & editing, Writing – original draft, Visualization, Validation, Supervision, Resources, Project administration, Methodology, Investigation, Funding acquisition, Formal analysis, Data curation, Conceptualization. **Kazuyuki Honma:** Visualization, Validation, Methodology, Investigation, Formal analysis. **Yukihisa Okumura:** Writing – review & editing, Visualization, Supervision.

Declaration of Competing Interest

The authors declare that they have no known competing financial interests or personal relationships that could have appeared to influence the work reported in this paper.

Acknowledgment

This work was partially supported by a Grant-in-Aid for Challenging Research (Exploratory) from Japan Society for the Promotion of Science (No. 18K18977) to D.S. Also, we gratefully acknowledge the work of past and present members of our laboratory.

Data availability

Data will be made available on request.

References

[1] N. Dolder, P. Müller, C. von Ballmoos, Experimental platform for the functional investigation of membrane proteins in giant unilamellar vesicles, Soft Matter 18 (2022) 5877–5893, https://doi.org/10.1039/D2SM00551D.
[2] D. Gaur, N.C. Dubey, B.P. Tripathi, Biocatalytic self-assembled synthetic vesicles and coacervates: from single compartment to artificial cells, Adv. Colloid Interface Sci. 299 (2022) 102566, https://doi.org/10.1016/j.cis.2021.102566.
[3] W. Jiang, Z. Wu, Z. Gao, M. Wan, M. Zhou, C. Mao, J. Shen, Artificial cells: past, present and future, ACS Nano 16 (2022) 15705–15733, https://doi.org/10.1021/acsnano.2c06104.
[4] P. Walde, K. Cosentino, H. Engel, P. Stano, Giant vesicles: preparations and applications, ChemBioChem 11 (2010) 848–865, https://doi.org/10.1002/cbic.201000010.
[5] T. Trantidou, M. Friddin, Y. Elani, N.J. Brooks, R.V. Law, J.M. Seddon, O. Ces, Engineering compartmentalized biomimetic micro- and nanocontainers, ACS Nano 11 (2017) 6549–6565, https://doi.org/10.1021/acsnano.7b03245.
[6] K. Shoji, R. Kawano, Recent advances in liposome-based molecular robots, Micromachines 11 (2020) 788, https://doi.org/10.3390/mi11090788.
[7] E. Rideau, F.R. Wurm, K. Landfester, Self-assembly of giant unilamellar vesicles by film hydration methodologies, Adv. Biosyst. 3 (2019) 1800324, https://doi.org/10.1002/adbi.201800324.
[8] L.M. Dominak, C.D. Keating, Polymer encapsulation within giant lipid vesicles, Langmuir 23 (2007) 7148–7154, https://doi.org/10.1021/la063687v.
[9] S. Pautot, B.J. Frisken, D.A. Weitz, Production of unilamellar vesicles using an inverted emulsion, Langmuir 19 (2003) 2870–2879, https://doi.org/10.1021/la026100v.
[10] S. Pautot, B.J. Frisken, D.A. Weitz, Engineering asymmetric vesicles, Proc. Natl. Acad. Sci. 100 (2003) 10718–10721, https://doi.org/10.1073/pnas.1931005100.
[11] M. Hadorn, E. Boenzli, P.E. Hotz, M.M. Hanczyc, Hierarchical unilamellar vesicles of controlled compositional heterogeneity, PLoS One 7 (2012) e50156, https://doi.org/10.1371/journal.pone.0050156.
[12] Y. Natsume, T. Toyota, Giant vesicles containing microspheres with high volume fraction prepared by water-in-oil emulsion centrifugation, Chem. Lett. 42 (2013) 295–297, https://doi.org/10.1246/cl.2013.295.
[13] K. Tsumoto, Y. Hayashi, J. Tabata, M. Tomita, A reverse-phase method revisited: rapid high-yield preparation of giant unilamellar vesicles (GUVs) using emulsification followed by centrifugation, Colloids Surf. Physicochem. Eng. Asp. 546 (2018) 74–82, https://doi.org/10.1016/j.colsurfa.2018.02.060.
[14] P. Taylor, C. Xu, P.D.I. Fletcher, V.N. Paunov, A novel technique for preparation of monodisperse giant liposomes, Chem. Commun. (2003) 1732–1733, https://doi.org/10.1039/B304059C.
[15] S. Matosevic, B.M. Paegel, Stepwise synthesis of giant unilamellar vesicles on a microfluidic assembly line, J. Am. Chem. Soc. 133 (2011) 2798–2800, https://doi.org/10.1021/ja109137s.
[16] K. Nishimura, H. Suzuki, T. Toyota, T. Yomo, Size control of giant unilamellar vesicles prepared from inverted emulsion droplets, J. Colloid Interface Sci. 376 (2012) 119–125, https://doi.org/10.1016/j.jcis.2012.02.029.
[17] Y. Ai, R. Xie, J. Xiong, Q. Liang, Microfluidics for biosynthesizing: from droplets and vesicles to artificial cells, Small 16 (2020) 1903940, https://doi.org/10.1002/smll.201903940.
[18] D.-Y. Li, Z.-H. Zhou, Y.-L. Yu, N.-N. Deng, Microfluidic construction of cytoskeleton-like hydrogel matrix for stabilizing artificial cells, Chem. Eng. Sci. 264 (2022) 118186, https://doi.org/10.1016/j.ces.2022.118186.
[19] C. Kurokawa, K. Fujiwara, M. Morita, I. Kawamata, Y. Kawagishi, A. Sakai, Y. Murayama, S.M. Nomura, S. Murata, M. Takinoue, M. Yanagisawa, DNA cytoskeleton for stabilizing artificial cells, Proc. Natl. Acad. Sci. 114 (2017) 7228–7233, https://doi.org/10.1073/pnas.1702208114.
[20] D.A. Fletcher, R.D. Mullins, Cell mechanics and the cytoskeleton, Nature 463 (2010) 485–492, https://doi.org/10.1038/nature08908.
[21] M. Weiss, J.P. Frohnmayer, L.T. Benk, B. Haller, J.-W. Janiesch, T. Heitkamp, M. Börsch, R.B. Lira, R. Dimova, R. Lipowsky, E. Bodenschatz, J.-C. Baret, T. Vidakovic-Koch, K. Sundmacher, I. Platzman, J.P. Spatz, Sequential bottom-up assembly of mechanically stabilized synthetic cells by microfluidics, Nat. Mater. 17 (2018) 89–96, https://doi.org/10.1038/nmat5005.
[22] K. Jahnke, V. Huth, U. Mersdorf, N. Liu, K. Göpfrich, Bottom-up assembly of synthetic cells with a DNA cytoskeleton, ACS Nano 16 (2022) 7233–7241, https://doi.org/10.1021/acsnano.1c10703.
[23] Y. Helwa, N. Dave, J. Liu, Electrostatically directed liposome adsorption, internalization and fusion on hydrogel microparticles, Soft Matter 9 (2013) 6151–6158, https://doi.org/10.1039/C3SM50837D.
[24] M. Grossutti, R. Seenath, S. Conlon, J.J. Leitch, J. Li, J. Lipkowski, Spectroscopic and permeation studies of phospholipid bilayers supported by a soft hydrogel scaffold, Langmuir 30 (2014) 10862–10870, https://doi.org/10.1021/la502925p.
[25] M. Grossutti, R. Seenath, J. Lipkowski, Infrared and fluorescence spectroscopic investigations of the acyl surface modification of hydrogel beads for the deposition of a phospholipid coating, Langmuir 31 (2015) 11598–11604, https://doi.org/10.1021/acs.langmuir.5b02813.
[26] M. Grossutti, R. Seenath, J.A. Noël, J. Lipkowski, Infrared and fluorescence spectroscopic studies of a phospholipid bilayer supported by a soft cationic hydrogel scaffold, J. Colloid Interface Sci. 473 (2016) 162–171, https://doi.org/10.1016/j.jcis.2016.03.055.
[27] A. Campbell, P. Taylor, O.J. Cayre, V.N. Paunov, Preparation of aqueous gel beads coated by lipid bilayers, Chem. Commun. (2004) 2378–2379, https://doi.org/10.1039/B406941B.
[28] A. Llopis-Lorente, M.J.G. Schotman, H.V. Humeniuk, J.C.M. van Hest, P.Y. W. Dankers, L.K.E.A. Abdelmohsen, Artificial cells with viscoadaptive behavior based on hydrogel-loaded giant unilamellar vesicles, Chem. Sci. 15 (2024) 629–638, https://doi.org/10.1039/D3SC04687G.
[29] D. Axelrod, D.E. Koppel, J. Schlessinger, E. Elson, W.W. Webb, Mobility measurement by analysis of fluorescence photobleaching recovery kinetics, Biophys. J. 16 (1976) 1055–1069, https://doi.org/10.1016/S0006-3495(76)85755-4.
[30] K. Makino, T. Yamada, M. Kimura, T. Oka, H. Ohshima, T. Kondo, Temperature- and ionic strength-induced conformational changes in the lipid head group region of liposomes as suggested by zeta potential data, Biophys. Chem. 41 (1991) 175–183, https://doi.org/10.1016/0301-4622(91)80017-L.
[31] M. Przybylo, J. Sýkora, J. Humpolíčková, A. Benda, A. Zan, M. Hof, Lipid diffusion in giant unilamellar vesicles is more than 2 times faster than in supported phospholipid bilayers under identical conditions, Langmuir 22 (2006) 9096–9099, https://doi.org/10.1021/la061934p.
[32] W.L.C. Vaz, R.M. Clegg, D. Hallmann, Translational diffusion of lipids in liquid crystalline phase phosphatidylcholine multibilayers. A comparison of experiment with theory, Biochemistry 24 (1985) 781–786, https://doi.org/10.1021/bi00324a037.
[33] L. Zhang, C.A. Booth, P. Stroeve, Phosphatidylserine/cholesterol bilayers supported on a polycation/alkylthiol layer pair, J. Colloid Interface Sci. 228 (2000) 82–89, https://doi.org/10.1006/jcis.2000.6910.
[34] T. Cha, A. Guo, X.-Y. Zhu, Formation of supported phospholipid bilayers on molecular surfaces: role of surface charge density and electrostatic interaction, Biophys. J. 90 (2006) 1270–1274, https://doi.org/10.1529/biophysj.105.061432.
[35] D. Saeki, T. Yamashita, A. Fujii, H. Matsuyama, A. Yamashita, H. Fujii, Matsuyama, Reverse osmosis membranes based on a supported lipid bilayer with gramicidin A water channels, Desalination 375 (2015) 48–53, https://doi.org/10.1016/j.desal.2015.07.030.
[36] D. Venturoli, B. Rippe, Ficoll and dextran vs. globular proteins as probes for testing glomerular permselectivity: effects of molecular size, shape, charge, and deformability, Am. J. Physiol. Ren. Physiol. 288 (2005) F605–F613, https://doi.org/10.1152/ajprenal.00171.2004.
[37] E.M. Ahmed, Hydrogel: preparation, characterization, and applications: a review, J. Adv. Res. 6 (2015) 105–121, https://doi.org/10.1016/j.jare.2013.07.006.